Int. Journ. of Peening Science and Technology, Vol. 1, pp. 75–86
Reprints available directly from the publisher.
Photocopying permitted by license only.

Effect of Different Ablative Overlays on Residual Stresses Introduced in IN718 SPF by Laser Shock Peening

ABHISHEK TELANG, AMRINDER S. GILL, GOKUL RAMAKRISHNAN AND VIJAY K. VASUDEVAN*

Department of Mechanical and Materials Engineering, University of Cincinnati, Cincinnati, OH 45221-0072, USA

Laser shock peening (LSP) was performed on IN718 SPF superalloy by using two different kinds of ablative overlays: a black vinyl tape and an Aluminum tape. The effect of ablative overlays on residual stresses induced by LSP was investigated. Two different power densities were used to peen the samples and in-depth residual stresses measured using conventional X-ray difraction (XRD).. Results show that Aluminum tape overlay introduced 100 to 150 MPa higher compressive residual stresses in the material as compared with the vinyl tape.

Keywords: Superalloys; laser shock preening; residual stresses; X-ray difraction (XRD); ablation overlays

1. INTRODUCTION

Laser shock peening (LSP) is a surface treatment process which is used to impart deep compressive residual stresses on surfaces of metallic components. LSP uses a high energy pulsed laser to ablate a thin opaque coating on the surface of the metal to be treated. Such pulses can instantaneously vaporize the surface layer into a high temperature (about 10,000 ^{o}C) and generate high pressure (up to several GPa) surface plasma [1]. The plasma formation absorbs all

*Corresponding author's e-mail: telangam@mail.uc.edu

the energy and blocks further transmission and prorogation of the laser beam. When this plasma blows away, it induces a shock wave into the material.

The direct ablation of materials causes plasma generation at the surface of the material/overlay. This plasma dissipates as soon as the laser pulse ends, it is not able to generate the high pressures required to create a shock wave. Hence, the plasma is confined by the use of a transparent overlay, usually glass or water. This confining media prevents the plasma from expanding away from the surface, allowing more time for deposition of laser energy and limits the expansion of plasma in the direction perpendicular to the surface of material. The effective length of the resultant pressure pulse generated is generally two to five times the duration of laser pulse and the peak pressure generated(up to tens of GPa) by this method can be up to 10 times higher compared to the direct ablation [2]. The shock wave deforms the near surface regions of the materials, introducing a non-uniform plastic deformation. The surrounding material and the subsurface material react to this, resulting in introduction of residual stresses in the near surface regions of the material.

During the laser interaction with a sample surface, the treated zone is dilated by the thermal effects and is then compressed by the surrounding matter, creating a compressive stress field. After the deposition time, the treated zone is restored by mechanical action of the untreated matter. The resulting surface residual stresses are consequently tensile stresses [3].

To avoid this problem, an overlay, opaque to the laser (typically black paint, tape or a variety of metallic tapes) is applied to the surface of the component being peened. This sacrificial layer is known as protective coating or ablative coating. It plays two roles: protecting the sample surface from thermal effects, as now no ablation of the material occurs and also it enhances the formation of plasma[4]. This helps in creating a pure mechanical effect in the material with no thermal effects. Although the advantages of using an opaque over lay are apparent, the process is time consuming as it involves a repetitive removal of overlay and cleanup of the surface. Some of the factors that can affect shock wave generation include thickness of the overlay, its laser interaction response and acoustic impedance[2]. A wide range of coating have been studied, including black paint, Al, Zn, Pb [5, 6]. In commercial applications, aluminum tape, black vinyl tape and black paint are predominantly used.

Fairand *et al.* [5] studied the pressure wave generated by various combinations of different transparent overlays (water and quartz) and ablative materials (black paint, Al and Zn). At lower power densities, Zn and black paint overlay generated higher pressures than Al. It was argued that thermal properties of the ablative layer played a role in magnitude of pressure generated. Acoustic impedance of overlay material was considered to play a much smaller role. Zn, with lower thermal conductivity could confine heat to interaction zone for longer durations while the higher conductivity aluminum lets the energy diffuse away. Zn also has low heat of vaporization, which means

that less energy goes into internal phase change and hence more energy is available for heating the plasma. The end result being Zn and black paint were able to generate pressure pulses of longer duration and higher magnitude than Al. At high power densities (>1 GW/cm^2), the choice of ablative material did not matter and generated similar peak pressures.

Similar results were obtained by Clauer *et al.* [6] in studying the plastic deformation produced in Fe-3 wt% Si alloy, by use of different overlays. In comparing use of no overlay, just plasma confining quartz overlay, just ablative Pb overlay and a combination of both confining quartz and ablative Pb layer. At lower power densities, combination quartz and ablative Pb layer lead to greatest deformation in the samples. The magnitude of deformation actually decreased with increased power densities. The reason for this was thought to be lower threshold for plasma formation in lead overlay, leading to plasma reflecting subsequent energy away from specimen.

Other studies by indicate that the thermal properties of overlay material are not as important Peyre and Fairand *et al*. [7, 8] concluded that different materials used for ablative overlays did not produce markedly different plasma pressures in the confined region. Their results indicate that enhanced pressure pulse getting transferred to the material is the consequence of acoustic impedance mismatch between two materials at the interface (ablative layer and the material being peened). They recorded a 30 to 50% enhancement is peak pressure, when a Al coating was used compared to no coating being used on 316L steel samples [9], which was attributed to impedance mismatch effect i.e when shock wave passes from material 1 to material 2, the pressure increases if $Z_1<Z_2$ (Z- Acoustic impedance)

The current study is limited to studying the effects of two different overlays for their effectiveness in producing compressive residual stresses in IN718 SPF. Tapes made of vinyl and Aluminum with adhesive backing were used. IN718 SPF alloy used in current study is a fine-grained Ni-base aero engine superalloy, capable of super plastic forming. This allows complex shapes to be produced that are otherwise difficult to achieve using conventional techniques. It is envisaged that ability to form complex parts by super plastic forming can reduce manufacturing costs.

2. EXPERIMENTAL DETAILS

The Inconel 718 SPF alloy used in current study was obtained from Special Metals Corporation in a sheet form of dimensions 250 x 250 mm^2 and thickness of 2 mm. The nominal composition of Alloy IN718SPF is given in Table 1.

The as-received sheet had been annealed and heat-treated to achieve AMS 5950 specifications for mechanical properties. Coupons of dimensions 38 x 38 x 2 mm^3 were sectioned from this sheet using electrical discharge machin-

TABLE 1
Nominal Chemical Composition (wt%) of IN718 SPF Alloy.

Ni	Cr	Nb	Mo	Al	Ti	C	Si	Mn	Cu	Fe
50-55	17-21	4.5-5.8	2.8-3.3	0.2-1.0'	0.3-1.3	0.1 (max)	0.75 (max)	0.5 (max)	0.75 (max)	Balance

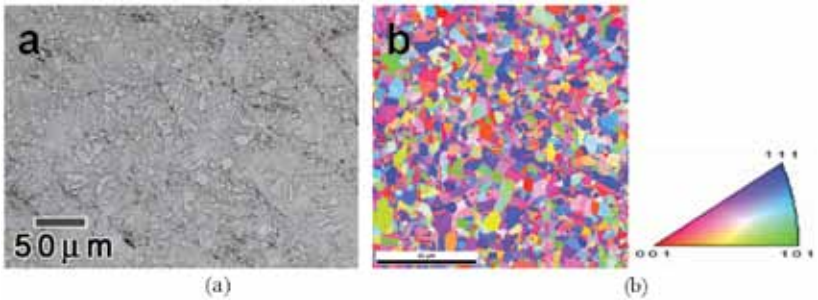

FIGURE 1
(a) Optical Micrograph and (b) IPF map of IN718 SPF.

ing (EDM). These coupons were then heat treated to 750 °C for 5 hours to remove any machining stresses and also to cause precipitation of γ'/γ'' to harden the material. For metallographic studies, a sample was polished to mirror finish. Part of polished sample was etched using a solution of 100 mL HCL and 0.5 mL H_2O_2 to perform optical microscopy. The same sample was also used for orientation imaging microscopy using Electron backs cattered Diffraction (EBSD).

Figure 1 shows the microstructure of the heat treated IN718 SPF alloy. The grain size was determined to be ~ 6 mm (ASTM 10 or higher). Figure 1(a) is an optical micrograph and Figure 1 (b) is the inverse pole figure (IPF) map obtained using Electron backscattered diffraction (EBSD)/ orientation imaging microscopy (OIM) in an FEI XL-30 scanning electron microscope (SEM). The IPF map suggests that grains are randomly oriented in the material. Fine grain size and absence of texture create good conditions for stress measurement by x-ray diffraction.

The LSP treatments were performed using a GEN I Q-switched Nd:Glass laser (wavelength = 1.053 µm.) at Ohio Center for Laser Shock Processing for Advanced Materials and Devices in University of Cincinnati. Samples were peened in a water confinement mode with following two conditions:

1. Energy=8.23 J, Pulse width=28.6 ns, spot size (diameter) = 2 mm, power density ~ 9 GW/cm^2.
2. Energy=15.24 J, Pulse width=25.3 ns, spot size=2.18 mm, power density ~16 GW/cm^2.

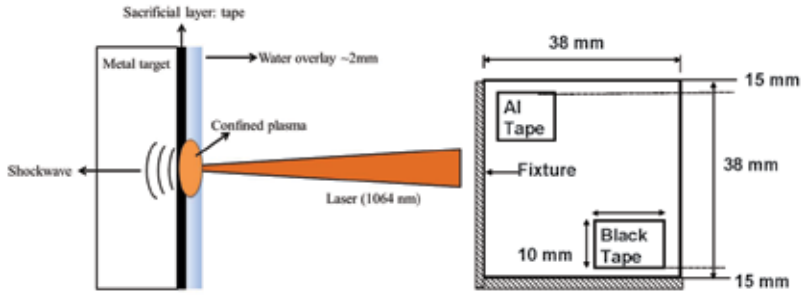

FIGURE 2
LSP schematic and sample geometry.

Two patches (one each with an overlay of Al tape and vinyl tape) of 10 mm x 10mm were LSP-treated from both sides, on each coupon, at diagonally opposite corners. A 15 mm distance was kept between patch and sample edges to avoid any edge effects while peening and subsequent stress measurements. Figure 2 shows the schematic of the LSP process and the sample geometry. The thickness of vinyl tape and Al tape was 130 μm and 60 μm respectively. The adhesive on the back, in both the tapes was 10-15 μm thick.

Residual stresses were analyzed at the center of each patch in two orthogonal directions using conventional X-ray diffraction (with $\sin^2\Psi$ technique) with electrolytic layer removal. Proto LXRD, a single axis goniometer using Ω geometry was used. Alignment of instruments was checked before each set of measurements using a standard sample (316 stainless steel powder in this case) in accordance with ASTM E915-96 ("Verifying the Alignment of X-ray Diffraction Instrumentation for Residual Stress Measurement").

To measure strains in depth, layer removal was done on the whole patch, using a solution of sulfuric acid and Methanol (12.5: 87.5% by volume). Fine layer removal was done in initial 50 μm depth (step size of ~5 μm), followed by a step size of 20 μm rest of the depth. This allowed for detailed mapping of stress fields in near surface regions. The data was corrected for stress gradients and layer removal. The X-ray elastic constants were measured in accordance with ASTM E1426-94 ("Determining the Effective Elastic Parameter for X-ray Diffraction Measurements of Residual Stress"). Detailed residual stress measurement parameters are provided in table 2.

3. RESULTS AND DISCUSSION

Laser shock peening introduced deep compressive residual stresses of high magnitude in all the conditions of this study. Figure 3 shows the Residual stress as a function of distance from peened surface for two power densities: 9 GW/cm^2 and 16 GW/cm^2, for two ablative coatings.

TABLE 2
XRD Parameters for Residual Stress Measurement.

Item	Description
Detector	PSSD (Position sensitive scintillation detector), 20^o 2θ range
Power	25 KV and 25 mA
Radiation	Mn $K\alpha_1$ ($\lambda = 2.10314A^o$)
Tilt angles	0^o, 2.58^o, 9.07^o, 12.45^o, 18.8^o, 23.0^o (Equal steps of $\sin^2 \psi$)
Aperture size(dia)	1 mm
Plane(Bragg's Angle)	{311} set of planes. Bragg's angle: 152^o
X-ray elastic constant	S2/2: 6.37 x 10^{-6} MPa^{-1}

The residual stresses were -56 MPa on the untreated material before LSP. In all cases, depth of compressive stress fields extended to around 550 to 600 mm deep from the treated surface. Clearly, in both energy conditions, Al tape overlay introduced higher compressive residual stresses in near surface regions than the black vinyl tape. For 9 GW/cm^2 condition, Vinyl tape overlay introduced a compressive stress of -580 MPa on surface while the Al tape introduced -810 MPa. Going further into depth, Al tape overlay shows stresses which are consistently 100-150 MPa higher in magnitude than those in case of vinyl tape. After a depth of 300 microns the vinyl tape profile showed a slightly higher compression. This could be due to the high compensating tensile stresses reducing the compressive stress values. Similar trends were seen in other orthogonal direction of measurements, so only results from only in-plane component are presented.

In 16 GW/cm^2 power density condition, the Al tape overlay produced ~ -800 MPa in near surface regions while Vinyl tape introduced ~ -680 MPa. In this case, the Al tape produced higher compression throughout the depth of compressive stress field (~ 600 μm). After 300 μm, the both stress profile come closer, as shock wave attenuates rapidly in nickel and hence plastic deformation caused on both cases becomes similar.

Diffraction peak FWHM gives an idea indication of lattice distortion (plastic strain) introduced in the material. Figure 4 shows the FWHM as a function of distance for all peening conditions. In both power densities, FWHM is higher for Al tape overlay. This indicates that plastic deformation introduced (and hence the peak pressure produced) is higher in case of Al overlay. Hence peak pressure in Al tape overlay must have been higher than in vinyl tape overlay.

For a given overlay, higher power densities also produced higher residual stresses. For Al tape overlay, power density of 9 GW/cm^2 introduced a maximum stress of ~-800 MPa and with 16 GW/cm^2, -860 MPa albeit a little below the surface. Similarly, for vinyl tape overlay, at 9 GW/cm^2 the maxi-

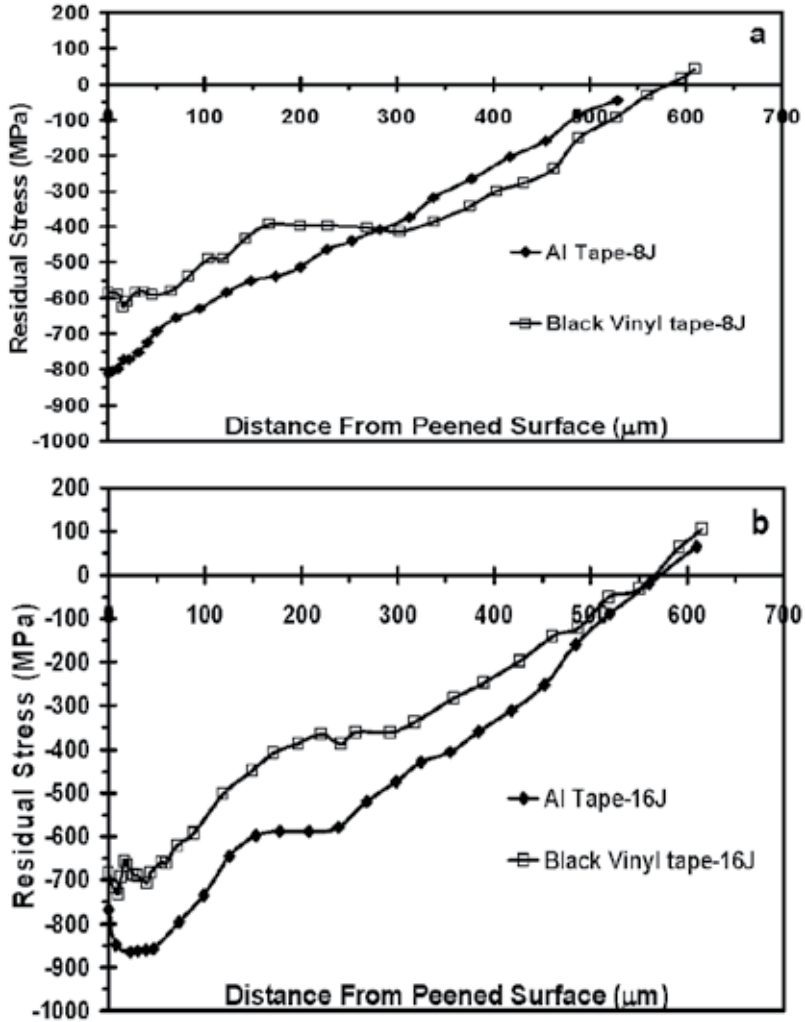

FIGURE 3
Residual stress *versus*. distance from peened surface for (a) 9 GW/cm^{2}condition and (b) 16 GW/cm^2 condition, for two ablative coatings.

mum stress introduced was -580 MPa and for 16 GW/cm^2 it increased to -680 MPa. The increase in magnitude of compressive residual stresses with increase in power density is seen. A similar trend can be observed in diffraction peak FWHM, with a higher power density inducing higher peak broadening due to the higher plastic deformation.

The magnitude of residual stresses and diffraction peak FWHM values for both power densities is not very different. This is due to the water (confinement layer) breakdown which happens at high power densities,

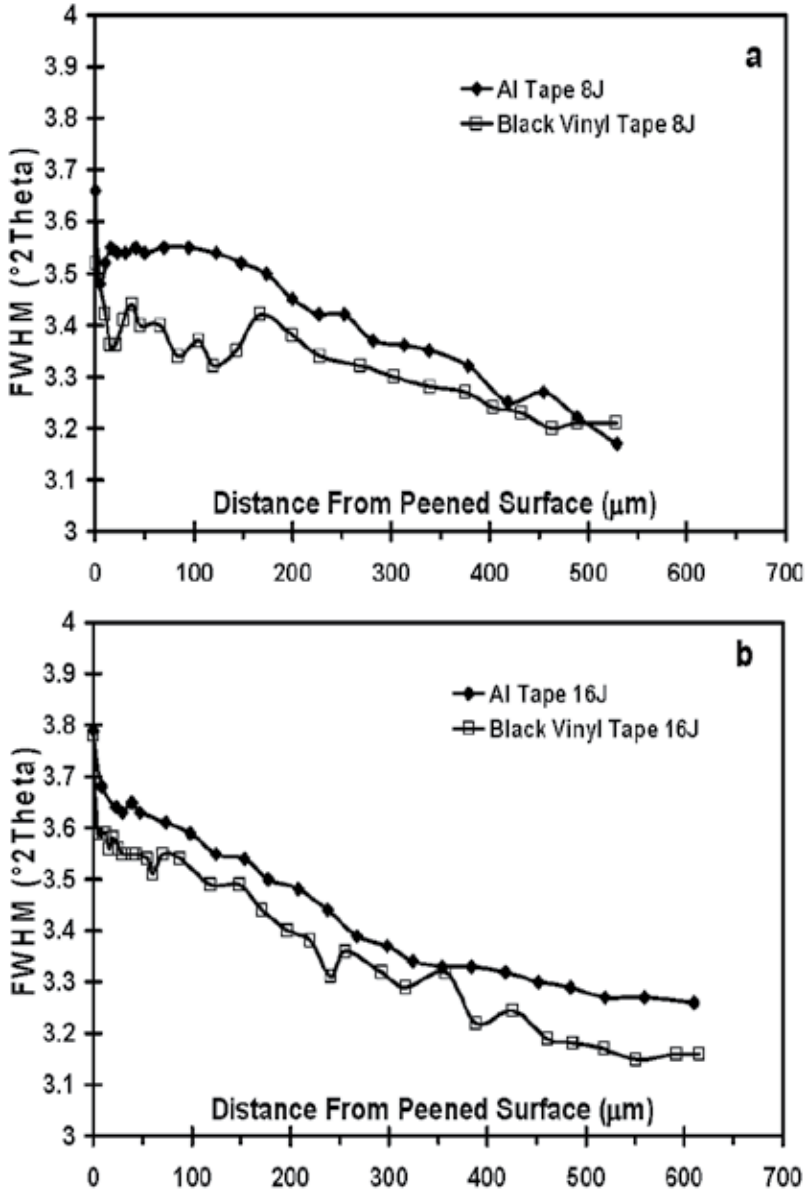

FIGURE 4
Diffraction peak FWHM *versus*. Distance from peened surface for (a) 8J energy condition and (b) 16J Energy condition, for two ablative layers

leading to formation of parasitic plasma at surface of water, leading to saturation of pressure pulse. The phenomenon has been observed and there are several studies available in literature [10-12]. Subsequent stud-

ies with our laser system have shown to achieve saturation pressure at power density of ~ 10 GW/cm^2. Hence, in the current study although the powers densities are very different, the pressure pulse generated by them must have been rather similar.

Fabbro *et al.* [13] modeled the confined ablation mode and related peak pressure of the plasma with laser power density. The relationship between peak plasma pressure and laser power density is given by

$$P(GPa) = 0.01\sqrt{\frac{\alpha}{2\alpha+3}} \bullet \sqrt{Z(g.cm^{-2}.s^{-1})} \bullet \sqrt{I_0(GW/cm^2)} \qquad (1)$$

where P is peak plasma pressure, I_o Incident laser power density, a Fraction of energy used in creating plasma (typically a=0.25 to 0.4)[12] and Z reduced shock impedance between metal component and target

Here Z is given by

$$\frac{2}{Z} = \frac{1}{Z_{Target}} + \frac{1}{Z_{Ablativeoverlay}} \qquad (2)$$

where Z_{Target} and $Z_{Ablative\ overlay}$ are the impedance of target and the ablative overlay in our case a black vinyl tape.

The acoustic impedance of vinyl is 0.25*10^6 g cm^{-2} S^{-1} [15] Aluminum is 1.45*10^6 g cm^{-2} S^{-1} [14] and that of the Nickel is 4.14*10^6 g cm^{-2} S^{-1} [14]. For vinyl tape-Nickel interface Z =0.4715*10^{6}g cm^{-2} S^{-1} and for Al tape-Nickel interface Z = 2.148*10^6 g cm^{-2} S^{-1}[14]. Clearly, Al tape should produce higher pressure pulse than a vinyl interface. As discussed earlier, acoustic impedance type mismatches result in pressure increase when transmitting shock waves from low acoustic impedance material to a high acoustic impedance material. Whenever there is a difference in acoustic impedances of the materials at an interface, some energy will be reflected. The fraction of energy that is reflected is given by the reflection coefficient, R:

$$R = \left[\frac{Z_2 - Z_1}{Z_2 + Z_1}\right]^2 \qquad (3)$$

where Z_1 and Z_2 are the acoustic impedances of the first and second material at an interface respectively. R for a vinyl-nickel interface comes to 0.75 and for an Al-Nickel interface is 0.23. Hence, Al-Ni interface is much more efficient at the energy transmission.

Another advantage of Al tape was that it did not spall or damage after one laser impact. The vinyl tape overlay was damaged after each impact and this necessitates leaving some space between successive laser shots. That means, the process has to be stopped to remove damaged tape, and clean the surface before a new tape is applied, in between peening sequences. In case of Al overlay, the tape was able to withstand up to two impacts at same location before damaging thus needing fewer changes of overlay in between sequences, making process faster.

4. CONCLUSIONS

Laser shock peening (LSP) was performed in a water confinement mode on IN718 SPF alloy using two different power densities (9 GW/cm^2 and 16 GW/cm^2) and two different ablative overlays: Al tape and a black vinyl tape. LSP introduced deep compressive stresses in all conditions, with depth of compression extending up to 600 μm from the peened surface. Al tape overlay was able to introduce substantially higher compressive stresses as compared to a vinyl tape overlay. This is due to the fact that a higher fraction of energy is reflected for the vinyl tape at the metal ablative layer interface, than the Al tape. So even though the vinyl tape has low heat of vaporization and hence should form plasma easier, it transmits lesser energy into the material than achieved by Al tape. Al tape was also able to last longer during processing, reducing processing time.

NOMENCLATURE

A_e	Energy coupling factor, <1
Cp	Specific heat at constant pressure (J/kgK)
d	Kerf depth (m)
h	Heat transfer coefficient (W/m^{2}K)
k	Thermal conductivity (W/mK)
L_{ev}	Latent heat of evaporation (J/kg)
M_w	Molecular weight of assisting gas (g/mol)
P	Power input in the workpiece (W)
P_g	Ni gas pressure (Pa)
P_0	Power input at the workpiece surface (W)
T	Temperature (K)
T_s	Surface temperature (K)
v	Laser beam cutting speed (m/s)
w	Laser beam waist diameter at workpiece surface (m)
w_k	Kerf width (m)
w_0	Beam waist diameter at surface when focus setting is nominal (m)

Greek symbols

β	Fraction of evaporation contribution, <1
ρ	Density of workpiece material (kg/m^3)
ρ_g	Density of assisting gas (kg/m^3)

ACKNOWLEDGEMENTS

The authors are grateful for financial support of this research by the Nuclear Energy University Program (NEUP) of the US Department of Energy contract #102835 issued under prime contract DE-AC07-05ID14517 to Battelle Energy Alliance, LLC. We also gratefully acknowledge the contribution of the State of Ohio, Department of Development and Third Frontier Commission, which provided funding in support of "Ohio Center for Laser Shock Processing for Advanced Materials and Devices" equipment in the Center that was used in this work. Any opinions, findings, conclusions, or recommendations expressed in these documents are those of the author(s) and do not necessarily reflect the views of the DOE or the State of Ohio, Department of Development.

REFERENCES

[1] Peyre, P., Fabbro, R., Berthe, L., and Dubouchet, C. Laser shock processing of materials, physical processes involved and examples of applications. *Journal of Laser Applications* **8** (1996), 135-141.

[2] Clauer, A.H., and Lahrman. D. F. Laser shock processing as a surface enhancement process. *Key Engineering Materials* **197** (2001), 121-144.

[3] Masse, J.-E., and Barreau, G. Laser generation of stress waves in metal. *Surface & Coatings Technology* **70** (1995), 231-234.

[4] Forget, P., Strudel, J.L, Jeandin, M., Lu, J., Castex, L. Laser shock surface treatment of Ni-based superalloys. *Materials and Manufacturing Processes* **5** (1990), 501-528.

[5] Fairand, B.P. and A.H. Clauer, Laser generated stress waves: Their characteristics and their effects to materials. *AIP Conference Proceedings* **50** (1979), 27-42.

[6] Clauer, A., B. Fairand, and B. Wilcox, Pulsed laser induced deformation in an Fe-3 Wt Pct Si alloy. *Metallurgical and Materials Transactions A* **8** (1977) 119-125.

[7] Peyre, P. Berthe, L., Scherperee, X., Fabbro, R. Laser-shock processing of aluminium-coated 55C1 steel in water-confinement regime, characterization and application to high-cycle fatigue behaviour. *Journal of Materials Science* **33** (1998) 1421-1429.

[8] Fabbro, R. Physics and applications of laser shock processing of materials. *Proceedings of SPIE - The International Society for Optical Engineering*. 2000. Osaka, Jpn: Society of Photo-Optical Instrumentation Engineers.

[9] Peyre, P., Fabbro, P., Berthe, L., Scherpereel, X., Bartnicki, E. Laser-shock processing of materials and related measurement, *High-Power Laser Ablation*, (1998), Santa Fe, NM, US.

[10] Peyre, P., Christelle, C., Arnault, S., Berthe, L., Caroline, R., de Los Rios, E.; Fabbro, Remy New trends in laser shock waves physics and applications. *Proceedings of SPIE - The International Society for Optical Engineering*. 2002.

[11] Devaux, D., Fabbro, R., Tollier, L., and Bartnicki, E. Generation of shock waves by laser-induced plasma in confined geometry. *Journal of Applied Physics* **74** (1993), 2268-2273.

[12] Fabbro, R., Peyre, P., Berthe, L., and Scherpereel, X. Physics and applications of laser-shock processing. *Journal of Laser Applications* **10** (1998), 265-279.

[13] Fabbro, R. Physical study of laser-produced plasma in confined geometry. *Journal of Applied Physics* **68** (1990) 775-784.

[14] Steinberg, D.J. *Equation of State and Strength Properties of Selected Materials*. 1996, Lawrence Livermore National Laboratory: Livermore, CA.

[15] Lees, S., Gilmore, R.S. and Kranz, P. R. Acoustic Properties of Tungsten-Vinyl Composites. *Sonics and Ultrasonics, IEEE Transactions* **20** (1973), 1-1.